

# **NON-DARCIAN CONVECTION FLOW IN A CIRCULAR DUCT PARTIALLY FILLED WITH POROUS MEDIUM**

**D.V.KRISHNA**

Department of Mathematics, Shirdi Sai Engineering College, Anekal, Bangalore.

## **ABSTRACT**

In this paper we discuss the flow and heat transfer in a circular duct bounded by a porous bed. The entire flow region is divided into two zones. Zone 1 consisting of clean fluid and Zone 2 consisting of porous bed. The clean fluid region is governed by Navier-Stokes equations while the Brinkman extended Darcy model has been used in the flow through porous bed. In either zones the momentum and temperature equations are coupled and in particular the equations in the porous region are non-linear coupled equations. In order to obtain a better incite into this complex problem we make use of Galarkian finite element analysis with quadratic polynomial approximations. The Galarkian finite element analysis has two important features, Firstly, the approximation solution is written directly as a linear combination of approximation functions with unknown nodal values as coefficients. Secondly, the approximation polynomials are chosen exclusively from the lower order piecewise polynomials restricted to contiguous elements. The behavior of the velocity and temperature is analyzed at different axial positions. The shear stress and the rate of heat transfer have also been obtained for variations in the governing parameters.

## **1. INTRODUCTION**

Convective heat transfer in channels partially filled with porous media has gained considerable attention in recent years because of its various applications in contemporary technology. These applications include porous journal bearing, nuclear reactors, porous flat plate collectors, packed bed thermal storage, solidification of concentrated alloys, fibrous and granular insulation, grain storage and drying, paper drying, and food storage. Besides, the use of porous substrates to improve forced convection heat transfer in channels, which is considered as a composite of a fluid and porous layers, finds applications in heat exchangers, chemical reactors, etc. Using the simple Darcy model, the fluid mechanics at the interface between the fluid layer and a porous medium over a flat plate was first investigated by Beavers and Joseph [1]. Later, this problem was investigated by Vafai and Thiyagaraja [7] analytically and obtained an approximate solution based on matched asymptotic expansions for the velocity and temperature distributions. Vafai and Kim [5] presented an exact solution

for the same problem. Excluding the microscopic inertial term, closed form analytical solutions for parallel plates and circular pipes partially filled with porous materials were obtained by Poulikakos and Kazmierczak [4] for constant wall heat flux, while numerical results were computed for constant wall temperature. Jang and Chen [3] investigated the problem of forced convection in a parallel plate channel partially filled with a porous material numerically. They used the Darcy- Brinkmann-Forchheimer model to derive the flow with in porous material.

Vafai & Kim [6] studied the interactions between the porous medium and the clear fluid simulated by the Darcy-Brinkman-Forchheimer formulation and the continuity of velocity and stresses at the interface and discussed the effects of several parameters, such as the porous layer thickness, the system configuration, Forchheimer coefficient, and Darcy number. The study includes the effects of these parameters on the transient thermal behavior of the channel under consideration.

Keeping above mentioned fact in view we discuss the flow and heat transfer in a circular duct bounded by a porous bed. The entire flow region is divided into two zones. Zone 1 consisting of clean fluid and Zone 2 consisting of porous bed. The clean fluid region is governed by Navier-Stokes equations while the Brinkman extended Darcy model has been used in the flow through porous bed. In either zones the momentum and temperature equations are coupled and in particular the equations in the porous region are non-linear coupled equations. In order to obtain a better incite into this complex problem we make use of Galarkian finite element analysis with quadratic polynomial approximations. The Galarkian finite element analysis has two important features, Firstly, the approximation solution is written directly as a linear combination of approximation functions with unknown nodal values as coefficients. Secondly, the approximation polynomials are chosen exclusively from the lower order piecewise polynomials restricted to contiguous elements. The behavior of the velocity and temperature is analyzed at different axial positions. The shear stress and the rate of heat transfer have also been obtained for variations in the governing parameters.

## **2.FORMULATION OF THE PROBLEM**

We consider free and forced convection flow in a vertical circular cylinder through a composite medium consisting of a clean fluid bounded by a coaxial porous matrix abutting the rigid cylindrical wall maintained at a constant temperature. The flow and temperature in the clean fluid (non porous) and porous regions are assumed to be fully developed. Both the fluid and porous region have constant physical properties and the flow is a mixed convection

flow taking place under thermal buoyancy and uniform axial pressure gradient. The boussenisq approximation is invoked so that the density variation is confined to the thermal buoyancy force. The flow in the clean fluid region is governed by Navier - Stokes equations, while the Brinkman – Forchhimer – Extended Darcy model which accounts for the inertia and boundary effects has been used for the momentum equation in the porous region. The clean fluid region is refer to as zone-1 and the porous region referred as zone-2. In both zone the momentum and energy equations are coupled and in particular the equation in the porous region is non-linear coupled equations. Also the flow in either zone is unidirectional along the axial direction of the cylinder. Making use of the above assumptions the governing equations the clean fluid region are

Zone – 1

$$-\frac{\partial p}{\partial z} + \mu\left(\frac{\partial^2 u}{\partial r^2} + \frac{1}{r} \frac{\partial u}{\partial r}\right) - \rho g = 0 \quad (\text{Equation of linear momentum}) \quad (2.1)$$

$$\rho c_p u \frac{\partial T}{\partial z} = \lambda\left(\frac{\partial^2 T}{\partial r^2} + \frac{1}{r} \frac{\partial T}{\partial r}\right) \quad (\text{Equation of energy}) \quad (2.2)$$

$$\rho - \rho_0 = -\beta g (T - T_0) \quad (\text{Equation of state}) \quad (2.3)$$

Where  $u$  is the velocity component of axial direction,  $T$  is a temperature of the fluid,  $p$  is pressure,  $\rho$  is the density of the fluid,  $k$  is permeability,  $c_p$  is specific heat at a constant temperature,  $\lambda$  is coefficient of thermal conductivity,  $\beta$  is the co-efficient of thermal expansion.  $\rho_0$  and  $T_0$  are the equilibrium density and temperature.

The corresponding equations in porous region are

Zone –2

$$-\frac{\partial p}{\partial z} + \frac{\mu}{\delta} \left(\frac{\partial^2 u_p}{\partial r^2} + \frac{1}{r} \frac{\partial u_p}{\partial r}\right) - \frac{\mu}{\delta} u_p - \frac{\rho \delta F}{\sqrt{k}} u_p^2 + \rho g \beta (T_p - T_0) = 0 \quad (2.4)$$

$$\rho c_p u_p \frac{\partial T_p}{\partial z} = \lambda \left(\frac{\partial^2 T_p}{\partial r^2} + \frac{1}{r} \frac{\partial T_p}{\partial r}\right) \quad (2.5)$$

Where  $u_p$  is the axial velocity in the porous region,  $T_p$  is the temperature of the fluid,  $k$  is permeability of medium,  $F$  is a function that depends on Reynolds number and the microstructure of the porous medium.

In zone-1 is the view of the symmetry with reference to the mid axis of the circular duct the symmetric condition are.

$$\left(\frac{\partial u}{\partial r}\right) = 0 \quad \& \quad \left(\frac{\partial T}{\partial r}\right) = 0 \quad \text{at } r = 0 \quad (2.6)$$

The boundary conditions relevant to the zone-2 are

$$u=0 \quad \& \quad T=T_1 \quad \text{at } r=a+s \quad (2.7)$$

In addition to these the following matching conditions at the fluid porous interface

$r= a$  are

$$u = u_p \quad \& \quad \frac{\partial u}{\partial r} = \frac{\partial u_p}{\partial r} \quad (2.8)$$

$$T = T_p \quad \& \quad \frac{\partial T}{\partial r} = \frac{\partial T_p}{\partial r} \quad (2.9)$$

The conditions (2.8) correspond to the continuity of the velocity and shear stress at the interface whereas the (2.9) corresponds continuity of the temperature and heat flux at the interface.

Introducing suitable non-dimensional variables in the governing equations in the non-dimensional form are (on removing the stars)

Zone-1 ( $0 \leq r \leq 1$ )

$$\frac{d^2 u}{d r^2} + \frac{1}{r} \frac{d u}{d r} = P - G \theta \quad (2.10)$$

$$\frac{d^2 \theta}{d r^2} + \frac{1}{r} \frac{d \theta}{d r} = P_r N u \quad (2.11)$$

Similarly the equations related to Zone-2 ( $1 \leq r \leq 1 + s$ )

$$\frac{d^2 u_p}{d r^2} + \frac{1}{r} \frac{d u_p}{d r} = P + \delta D^{-1} + \delta^2 \Lambda u_p^2 - \delta G \theta_p \quad (2.12)$$

$$\frac{d^2 \theta_p}{d r^2} + \frac{1}{r} \frac{d \theta_p}{d r} = P_r N u_p \quad (2.13)$$

Where

$$\Lambda = F D^{-1} \quad (\text{Inertia parameter or Forchhimer number})$$

$$G = \frac{g \beta (T_1 - T_0) a^3}{\gamma^2} \quad (\text{Grashoff number})$$

$$D^{-1} = \frac{a^2}{k} \quad (\text{Inverse Darcy Parameter})$$

$$N = \frac{A a}{T_1 - T_0} \quad (\text{Non - dimensional temperature gradient})$$

$$P_r = \frac{\rho c_p \gamma}{\lambda} \quad (\text{Prandtl number})$$

The corresponding non dimensional conditions are

$$\frac{du}{dr} = 0 \quad \& \quad \frac{d\theta}{dr} = 0 \quad \text{on } r = 0 \quad (2.14)$$

$$u_p = 0, \quad \theta_p = 1 \quad \text{on } r = 1 + s \quad (2.15)$$

The interfacial conditions are

$$u = u_p \quad \& \quad \frac{du}{dr} = \frac{du_p}{dr} \quad \text{at } r = 1 \quad (2.16)$$

$$\theta = \theta_p \quad \& \quad \frac{d\theta}{dr} = \frac{d\theta_p}{dr} \quad \text{at } r = 1 + s \quad (2.17)$$

### **3. FINITE ELEMENT ANALYSIS**

The finite element analysis with quadratic polynomial approximation functions is carried out along the radial distance across the circular duct. The behavior of the velocity and temperature profiles has been discuss computationally for different variation in governing parameters. The Gelarkin method has been adopted in the variational formulation in each element to obtain the global coupled matrices for the velocity and temperature in course of the finite element analysis.

Zone -1 ( $0 \leq r \leq 1$ )

Choosing different Lagranges quadratic polynomials  $\psi_{j=1,2,3}^k$  corresponding to each element  $e_k$  in zone-1 the local stiffness matrix of order 3x3 in term of local nodal values for the velocity in the form.

$$(a_{ij}^k)(u_i^k) - G(b_{ij}^k)(\theta_i^k) = (Q_{2j}^k) + (Q_{1j}^k) + (v_j^k) \quad (3.1)$$

Likewise local stiffness matrix of order 3x3 in term of local nodal values for the temperature in the form.

$$(c_{ij}^k)(\theta_i^k) - NP_r(d_{ij}^k)(u_i^k) = (R_{2j}^k) + (R_{1j}^k) \quad (3.2)$$

Where  $(a_{ij}^k), (b_{ij}^k), (c_{ij}^k) \& (d_{ij}^k)$  are 3x3 matrices. And  $(Q_{1j}^k), (Q_{2j}^k), (R_{1j}^k), (R_{2j}^k) \& (v_{1j}^k)$  are

3x1 column matrices and  $v_j^k = P \int_{r_{A_1}}^{r_{B_1}} r \psi_j^k dr$ .

Repeating the process with each of element  $e_k$  we obtain corresponding local stiffness matrices. These stiffness matrices are than assembled making use of inter element continuity

and equilibrium conditions to obtain the coupled global matrices for  $u$  &  $\theta$  in terms of global nodal values of  $u$  &  $\theta$  in zone -1. If the number of quadratic elements is chosen as  $n$  then the matrix will be order  $2n+1$ .

Zone-2 ( $1 \leq r \leq 1+s$ )

Choosing different Lagranges polynomials  $\psi_{jp}^k$ 's corresponding to each element  $e_k$  in zone-2 the local stiffness matrix of order  $3 \times 3$  for the velocity in the form

$$(f_{ij}^k)(u_{ip}^k) - \delta G(g_{ij}^k)(\theta_{ip}^k) + \delta D^{-1}(m_{ij}^k)(u_{ip}^k) + \delta^2 \Lambda(n_{ij}^k)(u_{ip}^k) = (Q_{2pj}^k) + (Q_{1pj}^k) + (v_{jp}^k) \quad (3.3)$$

Likewise the local stiffness matrix of order  $3 \times 3$  for the temperature in the form

$$(e_{ij}^k)(\theta_{ip}^k) - N P_r(t_{ij}^k)(u_{ip}^k) = (R_{2pj}^k) + R_{1pj}^k \quad (3.4)$$

Where  $(f_{ij}^k), (g_{ij}^k), (m_{ij}^k), (n_{ij}^k), (e_{ij}^k)$  and  $(t_{ij}^k)$  are  $3 \times 3$  matrices and  $v_j^k = -P \int_{r_{A_1}}^{r_{B_1}} r \psi_{ip}^k \psi_j^k dr$

and  $(Q_{2pj}^k), (Q_{1pj}^k), (R_{2pj}^k) \& (R_{1pj}^k)$  are  $3 \times 1$  column matrices .

Such stiffness matrices (3.3) & (3.4) in terms of local nodes in each element are assembled using interelement continuity and equilibrium conditions to obtain the coupled global matrices in terms of the global nodal values of  $u_p$  &  $\theta_p$  in zone-2. In case we choose  $n$  quadratic elements then the global matrices are of order  $2n+1$ . The coupled global matrices corresponding to zone-1 and zone-2 are again assembled using interface continuity conditions at the porous – non porous interface as well as the symmetric and boundary conditions. The ultimate coupled global matrices are solved to determine the unknown global nodal values of the velocity and temperature in both the clean fluid and porous regions. In solving these global matrices an iteration procedure has been adopted to include the boundary & effects in the porous region.

In fact, the non-linear term arises in the modified Brinkman linear momentum equation of the porous medium. The iteration procedure in taking the global matrices as follows. We split the square term into a product term and keeping one of them say  $U_{ip}$ 's under integration, the other is expanded in terms of local nodal values and the resulting in the corresponding co-efficient matrix  $(n_{ij}^k)$ 's in (3.3), whose coefficients involve the unknown  $U_{ip}$ 's . To evaluated (3.3) to begin with choose the initial global nodal values of  $U_{ip}$ 's as zeros in the zeroth approximation. We evaluate  $u_{ip}$ 's and  $\theta_{ip}$ 's in the usual procedure

mentioned earlier. Later choosing these values of  $u_{ip}$ 's as first order approximation calculate  $\theta_{ip}$ 's. In the second iteration, we substitute for  $U_{ip}$ 's the first order approximation of  $u_{ip}$ 's and the first approximation of and  $\theta_{ip}$ 's obtain second order approximation. This procedure is repeated till the consecutive values of  $u_{ip}$ 's and  $\theta_{ip}$ 's and differ by a preassigned percentage. For computational purpose we choose five elements in each zone.

Assembling the local stiffness matrices and using interelement continuity conditions in zone-

1. The global matrix for  $\theta$  in zone 1 is  $A_1 X_1 = B_1$  (3.5)

The global matrix for u in zone -1 is  $A_2 X_2 = B_2$  (3.6)

Similarly the global matrix for  $\theta_p$  in zone-2 is  $A_3 X_3 = B_3$  (3.7)

The global matrix for  $u_p$  is  $A_4 X_4 = B_4$  (3.8)

$A_1, A_2, A_3$  and  $A_4$  are constant coefficient matrices of order 11x11 and  $X_1, X_2, X_3, X_4, B_1, B_2, B_3$  &  $B_4$  are 11x1 column matrices.

We make use of the following interfacial and equilibrium conditions in term of global nodes are

$$u_{11} = u_{p_1} \text{ \& } \theta_{11} = \theta_{p_1} \quad (3.9)$$

The equilibrium conditions are

$$\begin{aligned} R_3^1 + R_1^2 = 0, \quad R_3^2 + R_1^3 = 0, \quad R_3^3 + R_1^4 = 0, \quad R_3^4 + R_1^5 = 0, \\ R_{p_3}^1 + R_{p_1}^2 = 0, \quad R_{p_3}^2 + R_{p_1}^3 = 0, \quad R_{p_3}^3 + R_{p_1}^4 = 0, \quad R_{p_3}^4 + R_{p_1}^5 = 0, \\ Q_3^1 + Q_1^2 = 0, \quad Q_3^2 + Q_1^3 = 0, \quad Q_3^3 + Q_1^4 = 0, \quad Q_3^4 + Q_1^5 = 0, \\ Q_{p_3}^1 + Q_{p_1}^2 = 0, \quad Q_{p_3}^2 + Q_{p_1}^3 = 0, \quad Q_{p_3}^3 + Q_{p_1}^4 = 0, \quad Q_{p_3}^4 + Q_{p_1}^5 = 0, \end{aligned} \quad (3.10)$$

The boundary conditions are

$$u_{p_{11}} = (u_p)_{r=1+s} = 0 \text{ \& } \theta_{p_{11}} = (\theta_p)_{r=1+s} = 1 \quad (3.11)$$

Assembling the temperature global matrices (3.5) in zone-1 and (3.7) in zone-2.

We obtain  $A_5 X_5 = B_5$  (3.12)

Similarly assembling global matrices for velocity (3.6) in zone-1 and (3.8) in zone-2 we obtain  $A_6 X_6 = B_6$  (3.13)

Where  $A_5$  &  $A_6$  are 21x21 square matrices  $X_5, X_6, B_5$  &  $B_6$  are 21x1 column matrices.

Solving these ultimate coupled global matrices for temperature and velocity (3.12) & (3.13) respectively and using the iteration procedure, we determine the unknown global nodes through which the temperature and velocity at different radial intervals at any arbitrary axial cross section are obtained. The respective expressions are given bellow

$$\begin{aligned}
\theta[r] &= 50\left(-\frac{1}{5} + r\right)\left(-\frac{1}{10} + r\right)\theta_1 - 100\left(-\frac{1}{5} + r\right)r\theta_2 + \\
& 50\left(-\frac{1}{10} + r\right)\theta_3 && 0 \leq r \leq 0.2 \\
& = 50\left(-\frac{2}{5} + r\right)\left(-\frac{3}{10} + r\right)\theta_3 - 100\left(-\frac{2}{5} + r\right)\left(-\frac{1}{5} + r\right)\theta_4 + \\
& 50\left(-\frac{3}{10} + r\right)\left(-\frac{1}{5} + r\right)\theta_5 && 0.2 \leq r \leq 0.4 \\
& = 50\left(-\frac{3}{5} + r\right)\left(-\frac{1}{2} + r\right)\theta_5 - 100\left(-\frac{3}{5} + r\right)\left(-\frac{2}{5} + r\right)\theta_6 + 50\left(-\frac{1}{2} + r\right) \\
& \left(-\frac{2}{5} + r\right)\theta_7 && 0.4 \leq r \leq 0.6 \\
& = 50\left(-\frac{4}{5} + r\right)\left(-\frac{7}{10} + r\right)\theta_7 - 100\left(-\frac{4}{5} + r\right)\left(-\frac{3}{5} + r\right)\theta_8 \\
& + 50\left(-\frac{7}{10} + r\right)\left(-\frac{3}{5} + r\right)\theta_9 && 0.6 \leq r \leq 0.8 \\
& = 50(-1+r)\left(-\frac{9}{10} + r\right)\theta_9 - 100(-1+r)\left(-\frac{4}{5} + r\right)\theta_{10} + 50\left(-\frac{9}{10} + r\right) \\
& \left(-\frac{4}{5} + r\right)\theta_{11} && 0.8 \leq r \leq 1
\end{aligned}$$

$$\begin{aligned}
\theta_p[r] &= \frac{50(-1+r-\frac{s}{5})(-1+r-\frac{s}{10})\theta_{11}}{s^2} - \frac{100(-1+r)(-1+r-\frac{s}{5})\theta_{12}}{s^2} + \\
&\frac{50(-1+r)(-1+r-\frac{s}{10})\theta_{13}}{s^2} && 1 \leq r \leq 1+s*0.2 \\
&= \frac{50(-1+r-\frac{2s}{5})(-1+r-\frac{3s}{10})\theta_{13}}{s^2} - \frac{100(-1+r-\frac{2s}{5})(-1+r-\frac{s}{5})\theta_{14}}{s^2} + \\
&\frac{50(-1+r-\frac{3s}{10})(-1+r-\frac{s}{5})\theta_{15}}{s^2} && 1+s*0.2 \leq r \leq 1+s*0.4 \\
&= \frac{50(-1+r-\frac{3s}{5})(-1+r-\frac{s}{2})\theta_{15}}{s^2} - \frac{100(-1+r-\frac{3s}{5})(-1+r-\frac{2s}{5})\theta_{16}}{s^2} + \\
&\frac{50(-1+r-\frac{s}{2})(-1+r-\frac{2s}{5})\theta_{17}}{s^2} && 1+s*0.4 \leq r \leq 1+s*0.6 \\
&= \frac{50(-1+r-\frac{4s}{5})(-1+r-\frac{7s}{10})\theta_{17}}{s^2} - \frac{100(-1+r-\frac{4s}{5})(-1+r-\frac{3s}{5})\theta_{18}}{s^2} + \\
&\frac{50(-1+r-\frac{7s}{10})(-1+r-\frac{3s}{5})\theta_{19}}{s^2} && 1+s*0.6 \leq r \leq 1+s*0.8 \\
&= \frac{50(-1+r-s)(-1+r-\frac{9s}{10})\theta_{19}}{s^2} - \frac{100(-1+r-s)(-1+r-\frac{4s}{5})\theta_{20}}{s^2} \\
&+ \frac{50(-1+r-\frac{9s}{10})(-1+r-\frac{4s}{5})\theta_{21}}{s^2} && 1+s*0.8 \leq r \leq 1+s
\end{aligned}$$

$$\begin{aligned}
u[r] &= 50\left(-\frac{1}{5} + r\right)\left(-\frac{1}{10} + r\right)u_1 - 100\left(-\frac{1}{5} + r\right)ru_2 + \\
&\quad 50\left(-\frac{1}{10} + r\right)ru_3 && 0 \leq r \leq 0.2 \\
&= 50\left(-\frac{2}{5} + r\right)\left(-\frac{3}{10} + r\right)u_3 - 100\left(-\frac{2}{5} + r\right)\left(-\frac{1}{5} + r\right)u_4 + \\
&\quad 50\left(-\frac{3}{10} + r\right)\left(-\frac{1}{5} + r\right)u_5 && 0.2 \leq r \leq 0.4 \\
&= 50\left(-\frac{3}{5} + r\right)\left(-\frac{1}{2} + r\right)u_5 - 100\left(-\frac{3}{5} + r\right)\left(-\frac{2}{5} + r\right)u_6 + \\
&\quad 50\left(-\frac{1}{2} + r\right)\left(-\frac{2}{5} + r\right)u_7 && 0.4 \leq r \leq 0.6 \\
&= 50\left(-\frac{4}{5} + r\right)\left(-\frac{7}{10} + r\right)u_7 - 100\left(-\frac{4}{5} + r\right)\left(-\frac{3}{5} + r\right)u_8 + \\
&\quad 50\left(-\frac{7}{10} + r\right)\left(-\frac{3}{5} + r\right)u_9 && 0.6 \leq r \leq 0.8 \\
&= 50(-1 + r)\left(-\frac{9}{10} + r\right)u_9 - 100(-1 + r)\left(-\frac{4}{5} + r\right)u_{10} + \\
&\quad 50\left(-\frac{9}{10} + r\right)\left(-\frac{4}{5} + r\right)u_{11} && 0.8 \leq r \leq 1
\end{aligned}$$

$$\begin{aligned}
u_p [r] &= \frac{50(-1+r-\frac{s}{5})(-1+r-\frac{s}{10})u_{11}}{s^2} - \frac{100(-1+r)(-1+r-\frac{s}{5})u_{12}}{s^2} \\
&+ \frac{50(-1+r)(-1+r-\frac{s}{10})u_{13}}{s^2} && 1 \leq r \leq 1+s*0.2 \\
&= \frac{50(-1+r-\frac{2s}{5})(-1+r-\frac{3s}{10})u_{13}}{s^2} - \frac{100(-1+r-\frac{2s}{5})(-1+r-\frac{s}{5})u_{14}}{s^2} + \\
&\frac{50(-1+r-\frac{3s}{10})(-1+r-\frac{s}{5})u_{15}}{s^2} && 1+s*0.2 \leq r \leq 1+s*0.4 \\
&= \frac{50(-1+r-\frac{3s}{5})(-1+r-\frac{s}{2})u_{15}}{s^2} - \frac{100(-1+r-\frac{3s}{5})(-1+r-\frac{2s}{5})u_{16}}{s^2} \\
&+ \frac{50(-1+r-\frac{s}{2})(-1+r-\frac{2s}{5})u_{17}}{s^2} && 1+s*0.4 \leq r \leq 1+s*0.6 \\
&= \frac{50(-1+r-\frac{4s}{5})(-1+r-\frac{7s}{10})u_{17}}{s^2} - \frac{100(-1+r-\frac{4s}{5})(-1+r-\frac{3s}{5})u_{18}}{s^2} \\
&+ \frac{50(-1+r-\frac{7s}{10})(-1+r-\frac{3s}{5})u_{19}}{s^2} && 1+s*0.6 \leq r \leq 1+s*0.8 \\
&= \frac{50(-1+r-s)(-1+r-\frac{9s}{10})u_{19}}{s^2} - \frac{100(-1+r-s)(-1+r-\frac{4s}{5})u_{20}}{s^2} + \\
&\frac{50(-1+r-\frac{9s}{10})(-1+r-\frac{4s}{5})u_{21}}{s^2} && 1+s*0.8 \leq r \leq 1+s
\end{aligned}$$

The shear stress are evaluated on the cylinder using the formula

$$\tau = \left( \frac{du}{dr} \right)_{r=1+s}$$

The rate of heat transfer ( Nusselt number ) are evaluated on the cylinder using the formula

$$Nu = - \left( \frac{d\theta}{dr} \right)_{r=1+s}$$

## 4. DISCUSSION

The velocity and temperature profiles, the shear stress and nusselt number are evaluated for variations in the governing parameters  $D^{-1}$ ,  $G$  and  $s$  at an arbitrary axial position of the circular duct. The influence of the thickness of the porous bed on the velocity, temperature in porous and clean fluid regions on the rate of heat transfer is also investigated. The different profiles for the variations in the governing parameters are drawn in Fig.1 – 10.

The velocity gradually reduces from its maximum attain on the mid axis of the duct to zero on the outer boundary in accordance with no – slip condition. We may note that, the thickness of the porous lining significantly affects the velocity and temperature in both the regions. Infact, for sufficiently large thermal buoyancy parameter ( $G \geq 10^2$ ), for an increase in the thickness of the porous bed, the magnitude of the velocity and temperature steeply enhances both in the clean fluid and the porous regions. In view of the non-dimensionalization the actual velocity may be obtained by scaling the non dimensional velocity by  $10^{-2}$ . The actual axial velocity is vertically downwards in view of the imposed pressure gradient chosen to be positive. Any upward flow corresponds to a reversal flow.

Figs.1 – 2 corresponds to variation of the velocity with reference to  $G$  and  $D^{-1}$  respectively, when the thickness of the porous bed 's' is small. Figs.3 – 4 correspond to the respective velocity profiles, when the thickness of the porous bed is large.

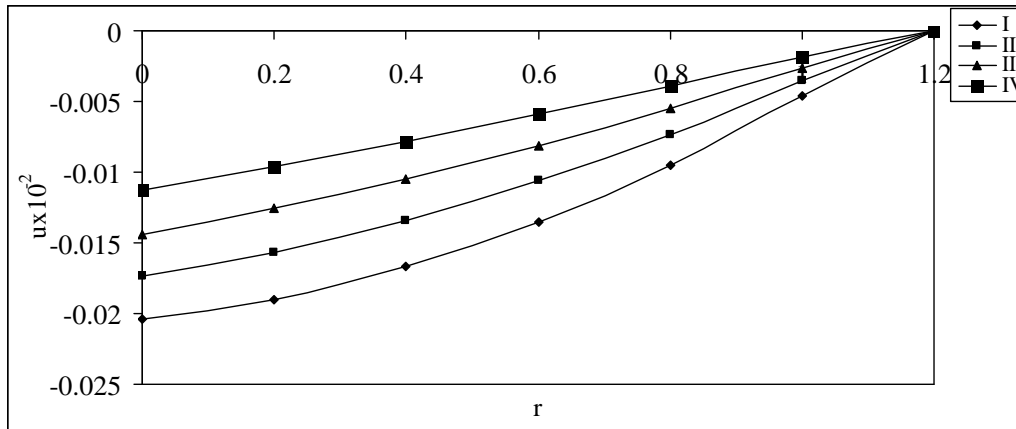


Fig1. Velocity  $u$  with  $G$  variation  $P=1$   $P_r = 7$   $N=0.5$   $d=0.001$   $D^{-1} = 1 \times 10^3$   $s=0.2$

	I	II	III	IV
G	50	100	150	200

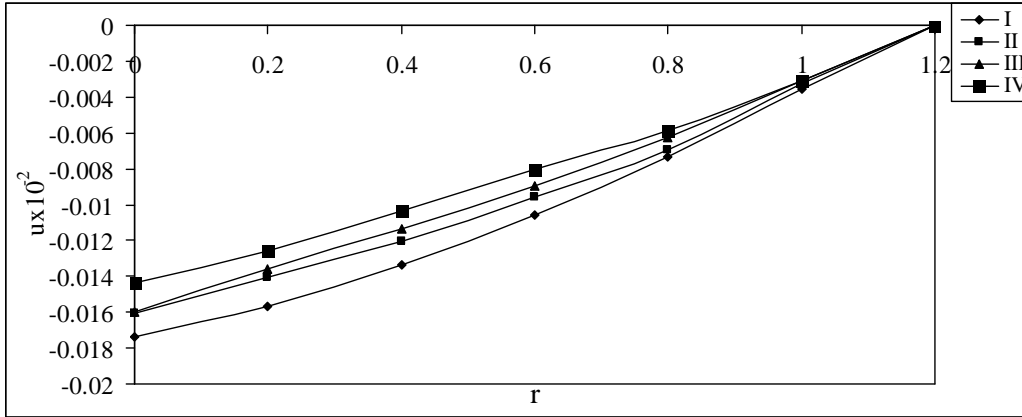


Fig2. Velocity u with G variation  $P=1$   $P_r = 7$   $N=0.5$   $d=0.001$   $G = 50$   $s=0.2$

	I	II	III	IV
$D^{-1}$	$10^3$	$2 \times 10^3$	$3 \times 10^3$	$4 \times 10^3$

From fig 1 we notice that when  $s$  is small an increase in the thermal buoyancy parameter  $G$  gradually reduces the axial velocity at all corresponding points in the fluid region (both clean and porous regions). Also from Fig 2, an increase in  $D^{-1}$  reduce the velocity in the clean fluid and slightly enhances the same in the porous bed. Thus as the permeability of the thin porous bed reduces, the fluid in the clean region moves with the lesser velocity. In contrast to this, when the thickness of the porous bed is large the axial velocity reduces with an increase in  $G$  through lower values ( $G \leq 10^2$ ).

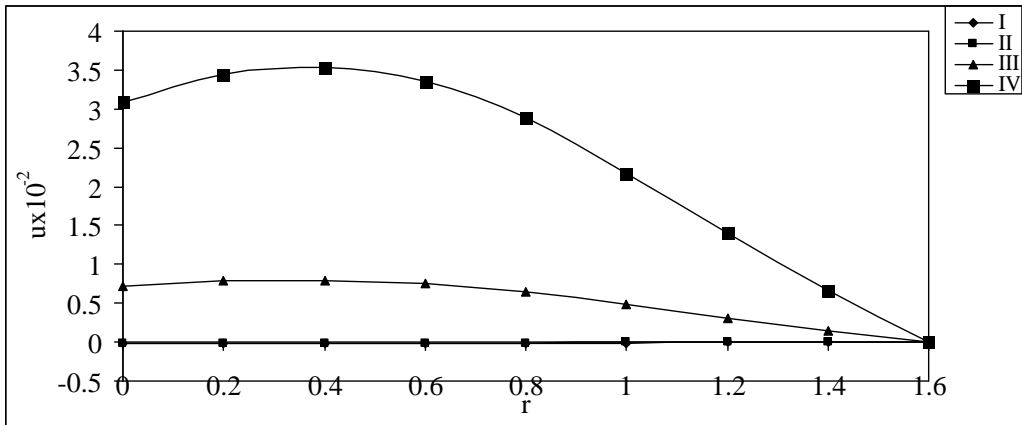


Fig3. Velocity u with G variation  $P=1$   $P_r = 7$   $N=0.5$   $d=0.001$   $D^{-1} = 1 \times 10^3$   $s=0.6$

	I	II	III	IV
G	50	100	150	200

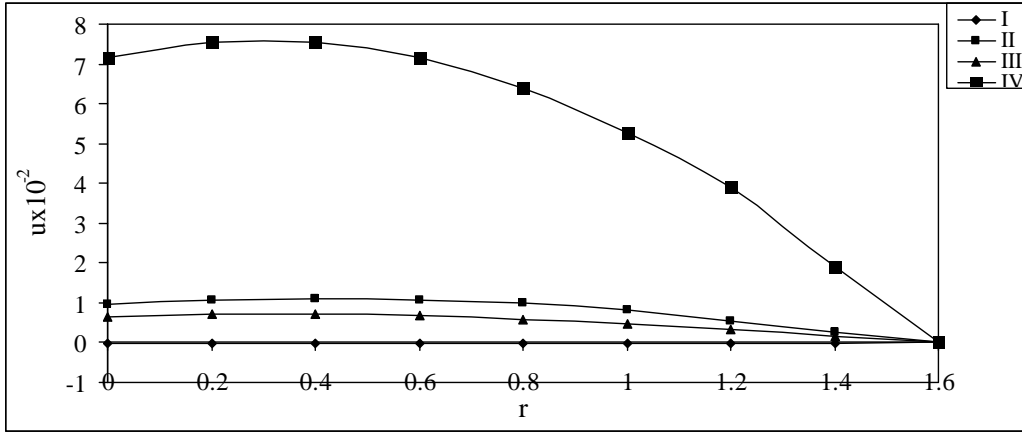


Fig4. Velocity  $u$  with  $D^{-1}$  variation  $P=1$   $P_r = 7$   $N=0.5$   $d=0.001$   $G = 50$   $s=0.6$

I	II	III	IV	
$D^{-1}$	$10^3$	$2 \times 10^3$	$3 \times 10^3$	$4 \times 10^3$

However when  $G$  enhances the velocity changes its direction and the magnitude steeply rises and higher the value of  $G$  greater the velocity. We also find that the velocity profiles are asymmetric parabolic with maximum attained at  $r=0.4$  (Fig.3). Fig.4 corresponds to the variation in the velocity with reference to  $D^{-1}$  and we find that an increase in  $D^{-1}$  through relatively small values ( $D^{-1} \leq 3 \times 10^2$ ) abruptly enhances the magnitude, which once again reduces for further an increase in  $D^{-1}$ . However the magnitude of the velocity once again sharply rises for further increase in  $D^{-1}$ .

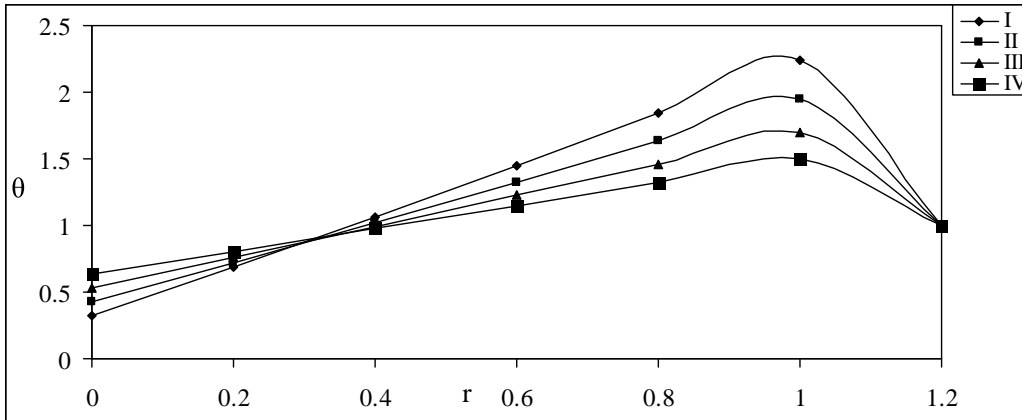


Fig5. Temperature  $\theta$  with  $G$  variation  $P=1$   $P_r = 7$   $N=0.5$   $d=0.001$   $D^{-1} = 1 \times 10^3$   $s=0.2$

I	II	III	IV	
$G$	50	100	150	200

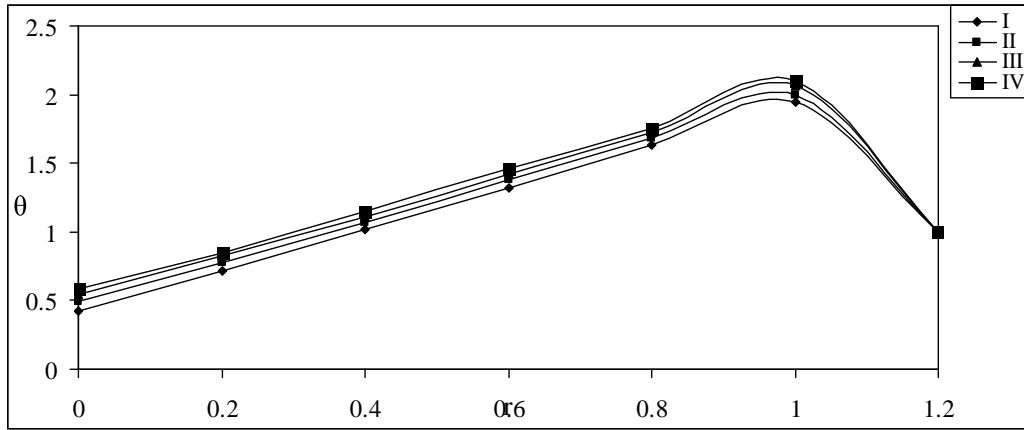


Fig6. Temperature  $\theta$  with  $D^{-1}$  variation  $P=1$   $P_r = 7$   $N=0.5$   $d=0.001$   $D^{-1} = 1 \times 10^3$   $s=0.2$

	I	II	III	IV
$D^{-1}$	$10^3$	$2 \times 10^3$	$3 \times 10^3$	$4 \times 10^3$

The behavior of the non- dimensional temperature in case of different thickness of the porous bed may be observed Figs 5-8. In the case of thin porous bed, the temperature enhances in magnitude is the core fluid region ( $0 < r < 0.4$ ) while reduces in the remaining fluid region including the porous bed, for an increase in  $G$ , keeping other parameters fixed (Fig5). The temperature slightly enhances in the entire region for an increase in  $D^{-1}$ . In other words, lesser the permeability of the porous medium higher the temperature in the fluid region (Fig6).

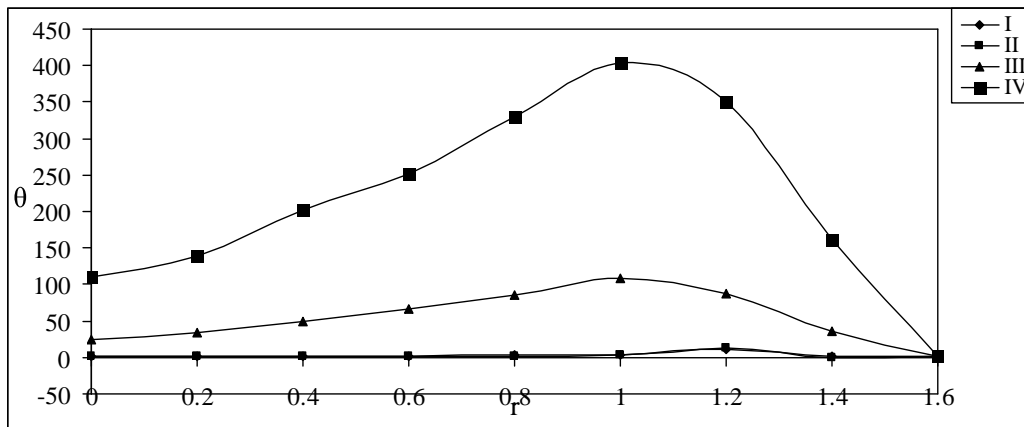


Fig7. Temperature  $\theta$  with  $G$  variation  $P=1$   $P_r = 7$   $N=0.5$   $d=0.001$   $D^{-1} = 1 \times 10^3$   $s=0.6$

	I	II	III	IV
$G$	50	100	150	200

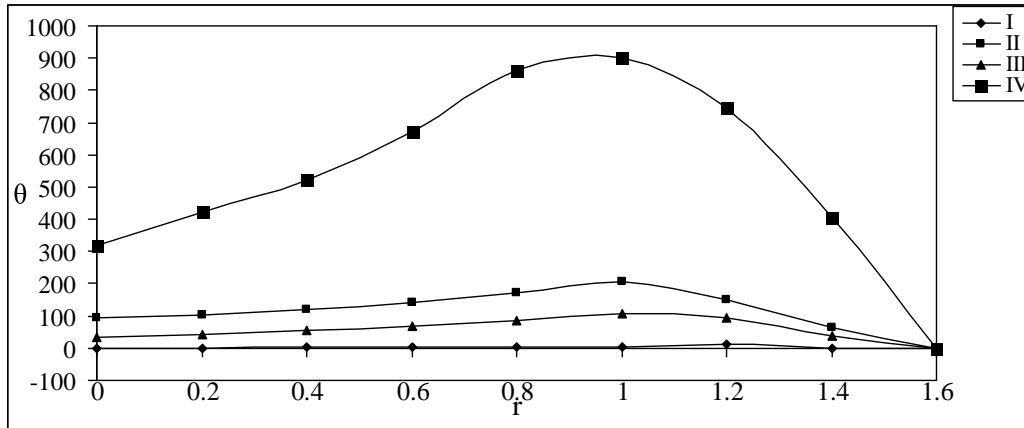


Fig8. Temperature  $\theta$  with  $D^{-1}$  variation  $P=1$   $P_r = 7$   $N=0.5$   $d=0.001$   $D^{-1} = 1 \times 10^3$   $s=0.6$

	I	II	III	IV
$D^{-1}$	$10^3$	$2 \times 10^3$	$3 \times 10^3$	$4 \times 10^3$

In case of porous bed of larger thickness, the temperature reduces for an increase in  $G$  through smaller values ( $G \leq 10^2$ ). Further an increase in  $G$  enhances the temperature at all corresponding points in the region (Fig7). A similar behavior is noticed with variation in  $D^{-1}$  (Fig8).

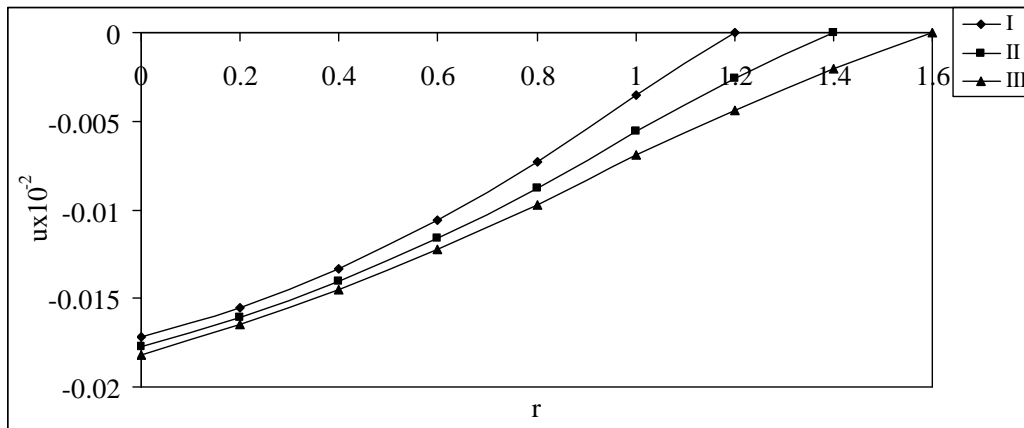


Fig9. Velocity  $u$  with  $s$  variation  $P=1$   $P_r = 7$   $N=0.5$   $d=0.001$   $G=50$   $D^{-1} = 1 \times 10^3$   $s=0.6$

	I	II	III
$s$	0.2	0.4	0.6

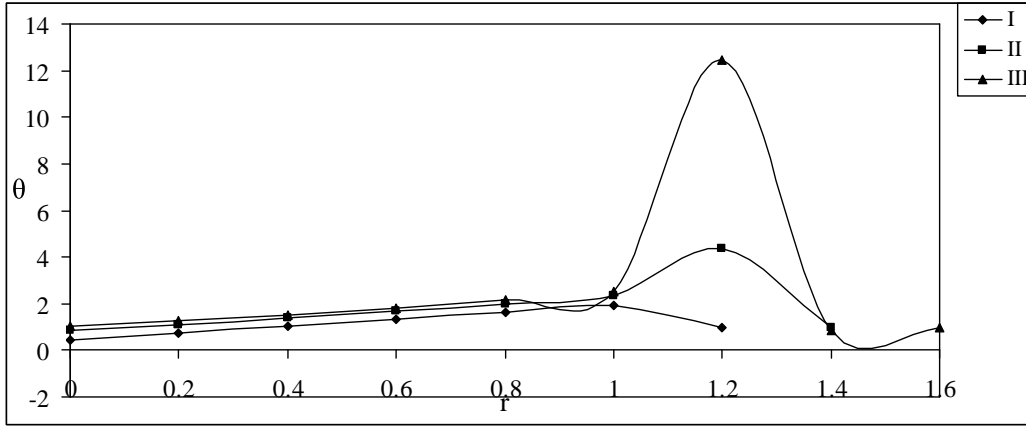


Fig10 Temperature  $\theta$  with s variation  
 $P=1 P_r = 7 N=0.5 d=0.001 G=50 D^{-1} = 1 \times 10^3 s=0.6$   

	I	II	III
s	0.2	0.4	0.6

Fig 9 indicates the variation in the velocity with enhancement of the thickness of the porous bed of the higher permeability. As pointed earlier, the fluid moves with enhanced velocity for increase in the thickness. Likewise, the temperature also enhances at all corresponding points in the entire region for an increase in thickness of the porous bed (Fig10).

Table-1

Shear Stress at the outer cylinder  $r=1+s$   
 $(P=1 P_r = 7 N=0.5 d=0.001 D^{-1} = 10^3 s=0.6)$

G=	50	100	150
s=0.4	1.9219	1.28889	0.861998
s=0.5	1.60712	1.12935	-76.7714
s=0.6	1.52836	1.05256	-574586

Table-2

Shear Stress at the outer cylinder  $r=1+s$   
 $(P=1 P_r = 7 N=0.5 d=0.001 G=50 s=0.6)$

$D^{-1} =$	$10^3$	$2 \times 10^3$	$3 \times 10^3$
s=0.4	1.83228	1.95451	2.09058
s=0.5	1.76881	1.95876	2.18527
s=0.6	1.75517	2.04408	2.41734

The shear stress is evaluated on the outer cylinder for different variations in the parameters and tabulated in tables 1 and 2. For smaller thickness of the porous bed an increase in G reduces the shear stress (Table1). For sufficiently large thickness the shear stress reduces with G for an increase through smaller values ( $G \leq 10^2$ ). But for further increase in G, the stress becomes negative and higher in magnitude. This is true for all large thickness of the bed. The changes in sign of the shear stress indicate the appearance of the reversal flow for higher values of G. From table-2 we notice that fixing G an increase in  $D^{-1}$  enhances the stresses for all thickness of the bed.

**Table-3**

Nusselt number at the outer cylinder  $r=1+s$   
 ( $P=1$   $P_r = 7$   $N=0.5$   $d=0.001$   $D^{-1} = 10^3$   $s=0.6$ )

G=	50	100	150
s=0.4	79.2557	78.0147	137.0802
s=0.5	63.8268	62.664	129.097
s=0.6	53.5265	52.3946	88.6656

**Table-4**

Nusselt number at the outer cylinder  $r=1+s$   
 ( $P=1$   $P_r = 7$   $N=0.5$   $d=0.001$   $G=50$   $s=0.6$ )

$D^{-1} =$	$10^3$	$2 \times 10^3$	$3 \times 10^3$
s=0.4	79.6192	80.0218	80.47
s=0.5	64.3529	64.9709	65.7072
s=0.6	54.2558	55.1831	56.3791

The rate of heat transfers for variation in  $s$  and  $D^{-1}$  has been obtained and tabulated in tables 3 & 4. For lower values of  $G$  reduces nusselt number for all thicknesses (Table3) but when  $G$  is large,  $Nu$  increases in magnitude. We also notice that higher the thickness of the bed lower the rate of heat transfer for all variations in  $G$  and  $D^{-1}$  (table 3). From table 4, we conclude that lesser the permeability of the medium higher the rate of heat transfers for all the values of  $s$  and  $G$ .

**5. REFERENCE**

1. Beavers, G.S and Joseph, D.D. : “Boundary conditions at a naturally permeable wall,”. Journal of Fluid mechanics, 13,197-207 (1967)
2. Chang W-J; Chang W-L : “Mixed convection in a vertical parallel-plate channel partially filled with porous media of high permeability”. Int J Heat Mass Transfer 39(7):1331-1342. (1996)
3. Jang JY; Chen JL : “Forced convection in a parallel plate channel partially filled with a high porosity medium.” Int Comm Heat Mass Transfer 19:263-273. (1992)
4. Poulikakos D; Kazmierczak M : “Forced convection in a duct partially filled with a porous material.” J Heat Transfer 109: 653-662. (1987)
5. Vafai,K and Kim, S.J : “Fluid mechanics of the interface region between a porous medium and a fluid layer-an exact solution”. International Journal of Heat and Fluid Flow, 11, 254-256 (1990)
- 6 Vafai,K and Kim, S.J., : “On the limitations of the Brinckman-Forchheimer-extended Darcy equation,”. International Journal of Heat and Fluid Flow,16,11-15 (1995)
7. Vafai.K. and Thiyagaraja, R : “Analysis of flow and heat transfer at the interface region of a porous medium,”. ”. International Journal of Heat and Mass Transfer,30,1391-1405 (1987).

This document was created with Win2PDF available at <http://www.win2pdf.com>.  
The unregistered version of Win2PDF is for evaluation or non-commercial use only.  
This page will not be added after purchasing Win2PDF.